Heliyon 5 (2019) e02186

Contents lists available at ScienceDirect

Heliyon

journal homepage: www.heliyon.com

Effect of Cutter Soil Mixing (CSM) method and curing pressures on the tensile strength of a treated soft clay

Parham Rabbani [a], Seyed Hamid Lajevardi [a,*], Ali Tolooiyan [b], Younes Daghigh [c], Mahroo Falah [d]

[a] Department of Civil Engineering, Arak Branch, Islamic Azad University, Arak, Iran
[b] School of Engineering, University of Tasmania, Hobart, TAS 7005, Australia
[c] Department of Civil Engineering, Karaj Branch, Islamic Azad University, Karaj, Iran
[d] Fibre and Particle Engineering, Faculty of Technology, University of Oulu, 90014, Oulu, Finland

ARTICLE INFO

Keywords:
Civil engineering
Cutter soil mixing
Stabilisation
Soft clay
Tensile strength
Curing pressure
Microstructure

ABSTRACT

This study presents a set of laboratory experiments to investigate the effect of Cutter Soil Mixing (CSM) method and curing pressures on the tensile strength of a soft clay treated with Air Cooled Blast Furnace Slag (ACBFS) and Industrial Hydrated Lime (IHL). High productivity, minimum vibration, using the in-situ soil as construction material, and high level of quality control are some of the main benefits of CSM method. Three different slurries containing various percentages of ACBFS and IHL were mixed with saturated soft clay due to CSM method to enhance its tensile strength and make it suitable for the construction of deep CSM panels. To simulate high pressure due to the self-weight of the deep CSM panels in the field, a number of high pressure curing devices were designed and built in the laboratory and used for 28 and 56 day pressurised curing of the treated samples. Then an indirect tensile strength test was performed on the treated samples to investigate the effect of mixing method, ACBFS-IHL content, curing pressure and curing time on the tensile strength of the treated material. Finally, X-Ray Diffraction (XRD) and Scanning Electron Microscopy (SEM) analysis were conducted to investigate the micro-structural and properties of the treated clay. The outcomes demonstrate that using CSM method and curing pressures along with ACBFS-IHL as a chemical stabiliser, increases the tensile strength of treated soft clay up to 35 times, which is significantly higher than the use of chemical stabiliser alone. Moreover, the microstructural analysis results revealed that the main hydration products in the clay treated with ACBFS-IHL is gismondine (C–A–S–H) which is also considered to be responsible for the higher tensile development.

1. Introduction

Problematic soft soils are located all over the world, in coastal, desert, alluvial, marsh and mud areas. Lack of sufficient bearing capacity, strength and stiffness are some of the obstructive elements limiting construction activities in these regions. Moreover, high porosity, excessive settlements, expansibility, swellability, collapsibility, dispersivity and liquefaction potential are additional challenges of these soils (Oliveira et al., 2011; Sargent et al., 2013, 2016; Jamsawanga et al., 2017). The main characteristics attributable to problematic soils relates to their composition, the nature of their pore fluids, their mineralogy and their fabric (Bell and Culshaw, 2001).

Intense weathering or hydrothermal conversion of alumina-silicate minerals can form clay minerals including kaolinite, illite and montmorillonite. Since these minerals are major components in sediments, rocks and soils, they can be considered as a main group of structural materials on the Earth (Moore and Reynolds, 1998; Zegeye et al., 2013). However, despite their wide distribution, the presence of soft clay minerals at construction sites is usually considered as a construction challenge.

Kaolin minerals consist of various phases such as quartz, micas and feldspars. In general, they are mined materials rich in kaolinite (Budhu, 2008). Kaolinite is the most abundant mineral in the soil, and is formed by chemical weathering of aluminium-silicates. The colour of kaolinite is white and has a considerable effect on the mechanical stability of soil column by interaction with other soil fabrics (Huertas et al., 1999; Chen et al., 2000). Low strength, high compressibility and low permeability are some of the main specifications of kaolin. Therefore, they generally exhibit low construction quality (Alrubaye et al., 2017). This type of problematic soft clay is a common material that can be found in the Middle East, Germany, France, United Kingdom, United States, China

* Corresponding author.
E-mail address: Sh-lajevardi@iau-arak.ac.ir (S.H. Lajevardi).

https://doi.org/10.1016/j.heliyon.2019.e02186
Received 19 January 2019; Received in revised form 13 February 2019; Accepted 26 July 2019

and Australia. According to project conditions, in most cases replacing this type of clay with suitable materials or carrying high-quality materials from other sources is not practically and economically possible. In these situations, choosing an appropriate method of soil improvement and stabilising with respect to the technical specifications leads to the improvement of engineering properties of the in-situ soil, which has a key role in project success from various aspects including timing, reliability and economical consideration.

Deep Mixing Method (DMM) is almost the most effective method for soft soil improvement, which has become very popular in recent years (Shen et al., 2008; Chai and Carter, 2011; Oliveira et al., 2011; Jamsawang et al., 2015; Wonglert and Jongpradist, 2015; Pi. Jamsawang et al., 2016a,b; Sargent et al., 2016; Güllü et al., 2017; Jamsawanga et al., 2017; Kitazume and Terashi, 2017). Cutter Soil Mixing is also a relatively new and very efficient technique for soil improvement, which is a subset of the DMM. CSM has several advantages compared with other DMMs, such as high level of process-quality control and quality assurance, making it advantageous to other deep mixing methods (Bellato et al., 2012). CSM panels are rectangular columns, which can be used in the form of earth retaining systems, construction foundation elements (piles and isolated columns) and cut-off walls (Gerressen and Vohs, 2012). Generally, some advantages such as low cost, no need of dewatering and fewer environmental risks have made deep soil mixing products useful in the form of retaining structures for deep excavation in soft soils. However, the low tensile strength of native and treated soils has always been a concern and has not been investigated well in relevant engineering literature (Shao et al., 2005; Arslan et al., 2008).

The allowable shear strength of the DMM product may be limited by its tensile capacity (Nicholson et al., 1998). ENREF62Recent investigations show that tensile strength should be taken into account in designing of composite earth retaining walls and laterally loaded piles (Saji and Numakarni, 1996; Denies et al., 2012; Xiaolin and Jiaa, 2012). This is due to the fact that tensile cracks develop in the composite structure if the generated bending moments force it in tension beyond its tensile strength (Rutherford et al., 2005; Shao et al., 2005). Several studies have also reported that external and internal failure can potentially occur in the Deep Mixed Columns (DMCs). Nguyen et al. (2016) showed that by using shallow layer of reinforcement, tensile cracks could initiate at surface layer connection or develop at the middle depth of DMCs under bending failure. Similar to other retaining structures, CSM panels may undergo tension during their construction or service life. Therefore, the tensile strength of the treated soil should be measured to achieve a reliable CSM retaining system. Lately more attention has been given to the tensile strength properties of soil as well as the development of new methods for improving soil tensile strength (Kitazume and Maruyama, 2007; Shindea et al., 2012; Li et al., 2014). Furthermore, the mean and principal stresses applied on stabilised soil masses differ from top (surface) to down (panel tip) in CSM walls. Therefore, determining the tensile strength of CSM panels by considering the influence of depth, and stresses generated by external structures is inevitable and has significant role in estimating the bearing capacity and reliability of CSM panels.

This paper presents the results of experimental investigation to evaluate the effec of Cutter Soil Mixing (CSM) method and curing pressures on improving the tensile strength of stabilised soft clay. In this process, a mixture of Air Cooled Blast Furnace Slag (ACBFS) and Industrial Hydrated Lime (IHL) were used as stabilisers for construction of shallow to deep CSM panels. Curing apparatuses were made in laboratory by adding in-house curing cells to modified oedometer frames to simulate the high pressure in-situ conditions and consolidate the prepared samples. Finally, to investigate the engineering properties of soil and additives from macro and micro point of view, a set of laboratory tests including indirect tensile strength, X-ray diffraction (XRD) and Scanning Electron Microscopy (SEM) were conducted on the treated samples that consist of various percentages of additives and cured under different curing pressures.

2. Background

2.1. Cutter soil mixing

The Cutter Soil Mixing (CSM) method is categorized as a subset of DMM. A modified trench cutter technique is used in this method to mix self-hardening slurries (cement slurry) with native in-situ soft soils. The first prototype CSM machine was built in 2003 (Bruce, 2009; Gerressen and Vohs, 2012). Until 2007, more than fifty projects were conducted in North America, New Zealand, Japan and Europe using this method, totalling about 1.4 million feet of panels (Bruce, 2009). CSM is mainly used for stabilising soft cohesive and non-cohesive soils (Bauer Maschinen GmbH, 2016). There are considerable differences between non-cohesive and cohesive soils considering the consistency and strength. Generally, cohesive soils are fine-grained materials, which have high clay or silt content. Therefore, cohesive soils exhibit significant effective cohesion as well as high plasticity and usually low strength. In contrast, non-cohesive soils are coarse-grain granular materials such as gravel and sand, which usually exhibit higher strength in compare with cohesive soils. Non-cohesive soils have none or negligible effective cohesion while their strength mostly depends on the friction in between soil particles (Wagner, 2013). This method is a Wet Rotary End (WRE) method with the rotating cutting wheels. To cut difficult and hard soils, wheels may be equipped by rock teeth (Brunner et al., 2006; Bellato et al., 2012; Gerressen and Vohs, 2012; Bruce et al., 2013). In general, the process of constructing CSM walls consists of several steps. The first step consists of positioning the cutter head in the wall axis. The second step breaks the soil matrix by driving the mixing tool including cutting wheels into the earth at constant rate while fluidifying slurry or compressed air is pumped through the wheel's nozzles to soften the soil and ease the process. After reaching the designed depth, the third step is the process of extracting the tools slowly while the self-hardening slurry is added to the softened soil continuously. Homogenization of the slurry and softened soil is guaranteed by rotations of the wheels. According to the project requirements, application purposes, and the final depth of construction, steel reinforced elements can be inserted into the constructed panel penetrating by their weight or by applying a light vibrator. This phase is considered as an optional step for the CSM project. CSM has many advantages in comparison with traditional soil mixing methods that use common rotary tools (Fiorotto et al., 2005). High productivity, no vibration during construction, little or no spoil (which is very important in contaminated areas), using in-situ soil as a construction material and reaching to 60m depth by using the rope suspended units are some other advantages of CSM (Bauer Maschinen GmbH, 2016).

2.2. Chemical soil stabilisation

According to the requirements of the project, different commercial stabilisers can be used for improving the engineering properties of fine-grained problematic soils. Different kinds of industrial by-products may be used to improve the strength properties of clayey soils. These kinds of materials or compounds improve the soft soil properties by activating pozzolanic reactions, ionic exchanges and flocculation of treated soil particles (Manso et al., 2013). Without a doubt, chemical stabilisation has the major role in the final quality of the CSM product. Chemical reactions caused by adding additives usually lead to changes in the native soil matrix from dispersed to flocculent structure, as well as increasing the soil strength parameters by binding the soil particles.

One of these additives is Blast Furnace Slag (BFS), which is a cheap and easy access non-metallic by-product. There are numerous iron and steel smelting factories around the world which produce significant amounts of such waste material during the iron and steel manufacturing process. Different types of slag are produced based on the methods used to cool the molten material. Air Cooled Blast Furnace Slag (ACBFS), Foamed Blast Furnace Slag (FBFS), Grand Granulated Blast Furnace Slag (GGBFS), and Pelletized Slag (PS) are some of these by-products (Bhuyan

and Singh, 2010). The majority of blast furnace slag produced around the world is air-cooled. BFS contains different minerals such as alumino-silicates, calcium alumino-silicates and silicates. This material is routinely used as an aggregate in other industrial products such as concrete, asphalt concerete, portland cement concerete, road bases and asphalt (FHWA-RD-97-148, 2016).

Crushed or milled cement-sized BFS particles with cementitious properties used as stabilizer. However, the slow reaction rate of the BFS causes using activators to proceed the reaction (Axelsson et al., 2002). One of the most successful and useful industrial stabilisers is lime, although, it takes months for lime treated soil to develop proper chemical reactions to reach an equilibrium state (Kabasy, 2013). On the other hand, BFS has moderate cementitious properties, therefore, it needs enough alkali to be chemically activated, which can be provided by hydrated lime (Higgins et al., 1998). The pozzolanic reactions of BFS with water and calcium hydroxide in alkali environments can result in a denser matrix with less porosity (Nazari and Riahi, 2011). The process of limestone burning leads to the production of lime. This chemical stabiliser can be added to the soil in different forms, such as quick lime (CaO) or hydrated lime ($CaOH_2$). A permanent strong cementitious matrix of lime treated soil can be achieved as a result of the reactions between soil particles and hydrated lime (Fiorotto et al., 2005). There are two major reactions when BFS and lime are mixed with a clayey soil, Calcium Alumino-Silicate Hydrate gel (C-A-S-H) and hydrotalcite type phases containing magnesium produced by the hydration of BFS activated by lime, while the reactions between lime and clay produce C–S–H, C-A-H and C-A-S-H (Abdel Rahman Ouf, 2001; Obuzor et al., 2012; Yi et al., 2015; Keramatikerman et al., 2016). Depending on the type and amount of BFS, additional calcium, alumino, silica and magnesia can be provided to the mixtures if higher percentages of BFS with only sufficient amount of lime is used (Regourd, 1980; Smolczyk, 1980; Obuzor et al., 2012; Yi et al., 2015). Generating such a ratio is also effective in preventing sulphate attack (Wild and Tasong, 1999; Higgins, 2005). Rahmat et al. (2016) observed that GGBFS-lime treated soil shows higher strength parameters in comparison with lime treated soil. It should be mentioned that the field mixing method and the economic considerations depending on the soil and stabiliser usually control the success of the stabilisation procedure (Mohamedzein et al., 2006).

2.3. Tensile strength

Measuring the tensile strength of materials is very important depending on their usage in engineering projects (Kabasy, 2013). The tensile strength of soft soil is negligible, hence, there is no widely accepted standard to determine the tensile strength of soft soils. However, the tensile strength of a soft soil may improve significantly after treatment and increases to the level of soft or even hard rock. Several methods can be used to determine the tensile strength of civil engineering materials, which can be split into two groups: direct and indirect methods (Li et al., 2014).

The Indirect tensile test is also called Brazilian or splitting test. In this test, a cylindrical sample is loaded by compressive distributed loads along two opposite flat or curved blocks. By applying the compressive load, the tensile failure occurs through a predetermined failure plan along the loading direction, where the sample fails in tension instead of compression. The highest force prior to the failure of the sample can be translated to its tensile strength (Kim et al., 2012).

The application of indirect tensile strength test in civil engineering is extensive. Tolooiyan et al. (2014) found this test useful for measuring the tensile strength of Intermediate Geotechnical Materials (IGM). This test is also suitable to evaluate the tensile specifications of treated soil mixtures (Thompson, 1965; Hudson and Kennedy, 1968). It should be noted that environmental changes such as temperature, moisture and compaction energy can also influence the tensile strength (Addanki et al., 1974; Fang, 1997). Although the right size of the sample as well as the possible effect of length to diameter ratio on the results is still being debated by researchers (Kim et al., 2012; Tolooiyan et al., 2014), the test is employed in this study as it is found suitable, considering the geometry of treated soil samples.

3. Materials and methods

3.1. Materials

In a common procedure, a mixture of cement and water (cement slurry) is added to the soil to chemically stabilise the considered volume of soil as a CSM panel. Air Cooled Blast Furnace Slag and Industrial Hydrated Lime are also eco-friendly inexpensive materials that can have the same function as cement with less environmental harm and energy consumption in process of production and use. Therefore, in this research, the mixtures of ACBFS and IHL are suggested as alternative materials to be applied in slurry form (ACBFS-IHL slurry) instead of cement slurry in the construction of CSM panels. Moreover, the finer particle size of additives associated with proper water to additive ratio, results a more fluid flow of slurry with an effect on its viscosity. To avoid the blockage of CSM device hoses and nozzles, which suggested by device manufacturer company (Bruce, 2009), fine grain additives (ACBFS-IHL) are prepared and the water to additives (water/ACBFS-IHL) ratio of one is applied in producing ACBFS-IHL slurry.

3.1.1. Clay

The problematic soil in this research is a kaolin classified among problematic soft clay, which located in Marand County, East Azerbaijan Province, Iran. Generally, fine grain soils with high moisture content and weak engineering properties such as high compressibility, low bearing capacity and strength which located in saturation condition near or below the phreatic surface are defined as problematic soft soils, that are merely capable of bearing their own weight and any additional loading will result in their large deformations (Kamon and Bergado, 1991; Kempfert and Gebreselassie, 2006). In order to confirm this, standard consolidation test and indirect tensile strength test were conducted to determine the compresibility and strength of the untreated soil due to ASTM standards (ASTM D2435/D2435M - 11, 2011; ASTM D3967 – 16, 2016). The compressibility index (Cc) of the untreated saturated soil was 0.3, while its tensile strength was negligible. To specify other geotechnical properties of this soft clay, hydrometer test, gradation test, specific gravity (Gs) test, Atterberg limits test and standatd proctor test were also performed based on ASTM standards (ASTM D422 – 63, 2007; ASTM D4318 – 10, 2010; ASTM D698 – 12, 2012; ASTM D854 – 14, 2014). Table 1 presents the geotechnical characterisation of tested clay. According to the test results, this clay is classified as a low plasticity clay. The particle size distribution of the clay is presented in Fig. 1.

The chemical composition of the clay was also determined by using X-Ray Fluorescence (XRF) test. It was observed that silicon dioxide (SiO_2) and aluminium oxide (Al_2O_3) are the main oxides composition of employed clay. Mentioned compositions play an important role in generation of C–S–H, C-A-H and even C-A-S-H gels during the process of

Table 1
Geotechnical properties of the untreated clay.

Geotechnical properties	Values
Specific gravity (G_S)	2.71
Plastic limit (%)	24.1
Liquid limit (%)	41
Plasticity Index (%)	16.9
Unified soil classification (UCS)	CL
Soil initial moisture content (%)	39
Saturated unit weight (kN/m^3)	17.3
Dry unit weight (kN/m^3)	12.4
Optimum moisture content (%)	24.3
Maximum dry unit weight (kN/m^3)	14.6
Compressibility index (Cc)	0.3
Tensile strength (kN/m^2)	Negligible

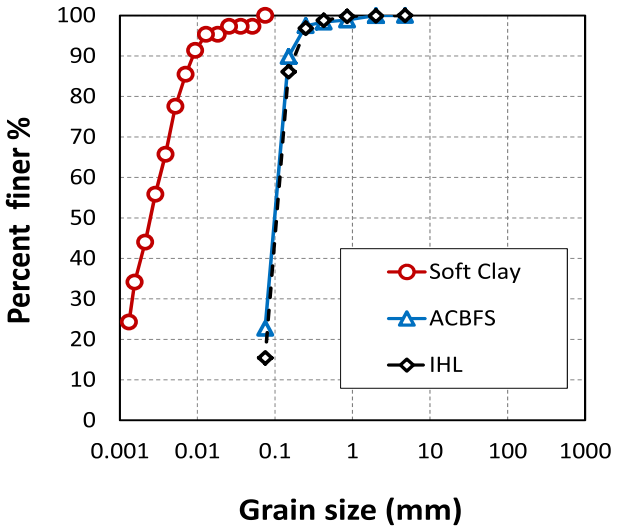

Fig. 1. Particle size distribution of the untreated clay, ACBFS and IHL.

chemical soil stabilisation (see Table 2).

3.1.2. Air cooled blast furnace slag (ACBFS)

The ACBFS used in this study is supplied by a local steel construction factory. It is widely accepted that by pouring the molten slag into beds and cooling it under ambient conditions a crystaline hard lump structure is produced called air cooled blast furnace slag. This hard lump structure can be crushed, milled and sieved (FHWA-RD-97-148, 2016). To improve the mixing efficiency, the ACBFS used in this research is crushed and softened by an industrial mill machine. After milling, specific gravity test and gradation test were conducted based on ASTM standards (ASTM D422 – 63, 2007; ASTM D854 – 14, 2014). The chemical composition of ACBFS was also determined using an XRF test. The obtained results showed that the specific gravity of ACBFC was 2.79 while the particle size distribution of ACBFS indicated that almost 90% of particles were finer than 0.15 mm (sieve No.100) and 23% were finer than 0.075 mm (sieve No.200). The particle size distribution and chemical composition of the ACBFS are presented in Fig. 1 and Table 3, respectively.

3.1.3. Industrial hydrated lime (IHL)

The process of producing hydrated lime (CaOH2) controls its purity. In the traditional production process, the purity of hydrated lime could reach up to 70% by simply adding water to quicklime (CaO). However, by using a newer technology of industrial hydration devices and blowing 300 to 400 centigrade steam to quicklime, the purity of final product (CaOH2) can reach 98%.

The industrial hydrated lime (IHL) used in this research is classified as high-grade hydrated lime with 92% purity and supplied by a local lime factory in East Azerbaijan Province, Iran. The specific gravity of IHL was determined 2.46 due to ASTM standard (ASTM D854 – 14, 2014). As illustrated in Fig. 1, the particle size distribution of the IHL indicated that almost 86% of particles were finer than 0.15 mm (sieve No.100) while 15.5% were finer than 0.075 mm (sieve No.200). Moreover, the chemical composition of IHL used in this study was determined by XRF testing, with results presented in Table 4.

Table 2
Chemical composition of the untreated clay.

Oxide Composition	Values
SiO_2	65 ± 1 %
Al_2O_3	22 ± 1 %
Fe_2O_3	0.75 ± 0.1 %
CaO	1.5 ± 0.2 %
Na_2O	0.35 ± 0.05 %
K_2O	0.25 ± 0.05 %
MgO	0.35 ± 0.05 %
TiO_2	0.04 ± 0.01 %
L.O.I	8.5 ± 1 %

Table 3
Chemical composition of the ACBFS.

Oxide composition	Values
SiO_2	50.85 %
Al_2O_3	10.65 %
Fe_2O_3	18.78 %
CaO	1.03 %
Na_2O	1.55 %
K_2O	1.33 %
MgO	0.11 %
TiO_2	0.612 %
MnO	15.63 %
P_2O_5	0.012 %
S	0.013 %
L.O.I	0.01 %

3.2. Testing apparatus

As one of the objectives of this research is to investigate the effect of curing/overburden pressure (depth of CSM panel) on the tensile strength of the treated soil, curing the samples in atmospheric pressure is not suitable. Hence, to simulate the field stress conditions, ten oedometer cells were modified as suggested by Tolooiyan and Gavin (2011) (see Fig.2 and 3b). By using the modified oedometer, the vertical load can be applied on the samples using 10:1 lever arm ratio, which amplifies the load by the factor of 10.

The mixture of soil and additives (ACBFS-IHL slurry) that has a paste form is poured into transparent plexiglas cylindrical moulds with 130 mm height and 50 mm internal diameter, to assure the final product has the minimum height/diameter ratio of 2 after consolidation and curing (ASTM D1633 - 00, 2007; ASTM D2166 - 16, 2016). To remove large bubbles of air and minimize the entrapped air from the paste, the outsides of the moulds were tapped lightly until the surface voids were closed. Moreover, transparent plexiglas helps to assure the samples are free from large air bubbles and voids while filling the cylinders with the mixtures (paste of soil and additives). To keep the samples wet during the consolidation and curing phase, all the cells were modified with longer fixing rods and taller water baths (see Fig. 3). The pours stones were placed at both ends of the samples to allow double drainage under curing pressure and during 28 and 56 days curing time. Therefore, water could escape the sample through upper and lower permeable boundaries to dissipate the excess pore water pressure generated during the loading period and to facilitate the samples consolidation. The porous disks were kept in clean water before conducting the test to saturate the porous stones and keep the pores clean to prevent from interruption of the flow and drainage.

Table 4
Chemical composition of the IHL.

Oxide composition	Values
$CaOH_2$	>92 %
SiO_2	<1 %
Al_2O_3	<0.5 %
Fe_2O_3	<0.2 %
CaO (free)	<1.5 %
Na_2O	<0.1 %
K_2O	<0.1 %
MgO	<0.1 %
MnO_2	<0.02 %
P_2O_5	<0.05 %
SiO_2 + insoluble materials	<1.3 %
SO_3	Trace

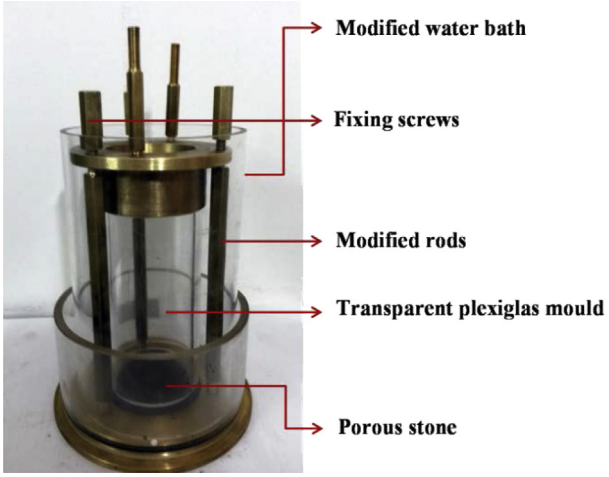

Fig. 2. Modified oedometer cell.

To estimate the tensile strength of the treated material based on the Brazilian tensile strength test method, a standard unconfined compression device was modified to suit the purpose. The Brazilian tensile strength testing device consists of two disks in the same axis located above and below a cylindrical sample (Kim et al., 2012; ASTM D3967 – 16, 2016). To reduce the concentration of contact stresses, two curved bearing blocks are used instead of flat discs. The width of contact between the curved blocks and the sample should be less than $D/6$, where D is the diameter of the sample. It should be noted that the sample diameter D must be equal or greater than ten times the size of the largest mineral grain constituent (ASTM D3967 – 16, 2016). The width of contact in this study was set to 8 mm, satisfying the $D/6$ criteria while D is 50 mm and considerably greater than ten times of the largest clay particle.

3.3. Samples preparation and testing program

In the process of preparing samples to represent the soft soil site, which is mostly wet and semi/fully saturated, water was added to the untreated dry clay to increase the moisture content to 95% of the clay liquid limit. The paste clay was then left in sealed containers for 24 h to ensure the even distribution of moisture content. To prepare the ACBFS-IHL slurry, in three separate containers, additives including ACBFS and IHL were mixed together in three different weights while maintaining the ACBFS:IHL ratio of 4:1. The ACBFS was added in 4, 12, and 20 %, while IHL was added in 1, 3 and 5% of the dry weight of untreated clay. Finally, to produce the ACBFS-IHL slurry, water was added to all the ACBFS-IHL mixtures and they were mixed for 5 min using a soil stirrer with a rotation speed of 10000 rpm. As discussed above, the ratio of water to ACBFS-IHL mixtures was 1:1 (see section 3.1). It should be noted that the role of IHL in this study is to be an activator for chemical reaction rather than being the main stabiliser. Previous investigations found that the 5:1 BFS:lime ratio is proper to activate BFS (Wild and Tasong, 1999; Rabbani et al., 2012), however, the 4:1 ratio was preferred in this study to assure all ACBFS will be activated and to minimise the ACBFS content.

The ACBFS-IHL slurry was mixed with the paste clay until homogeneous and uniform in colour. Finally the mixture was poured into plexiglas moulds and placed inside the oedometer cell to be loaded. In total, thirty samples were prepared consisting of various percentages of additives as previously detailed. All the samples were named as SxAyHz, where, S, A and H denote soil, ACBFS, IHL, respectively. The x, y and z indexes represent the final moisture content of the sample, percentage of ACBFC, and IHL, respectively. The details of prepared samples are shown in Table 5.

Similar research has mainly focused on the behaviour of treated soils cured in atmospheric pressure. However, in this research, to investigate the effect of curing pressure induced by the weight/depth of CSM panel and confining soil, twenty four cylindrical samples were cured under 100kPa, 200kPa, 300kPa and 400kPa curing pressure (also called overburden pressure), with six samples cured at atmospheric pressure. To investigate the effect of curing time, the samples were tested after 28 and 56 days. From the practical and construction management point of view, 28 and 56 days curing periods are acceptable time frames for most construction projects. Moreover, usually 28–56 days of curing is suitable time for most pozzolanic reactions to happen and formation of cementitious material, which has influence on increasing the strength parameters of the treated soil (Nelson and Miller, 1992; Bruce, 2009; Bruce et al., 2013). The room temperature was set to 25 °C during sample preparation and testing. Fig. 3 shows the prepared sample before and after curing.

At the end of curing time, samples were extruded from the plexiglas moulds using a hydraulic jack. After extruding, to make the required sample geometry suggested by ASTM standard (ASTM D3967 – 16, 2016), all the cylindrical samples were cut into 5 Brazilian test disks with 20 mm thickness, 50 mm diameter, providing a disk thickness-to-diameter ratio (t/D) of 0.4. Finally, the samples disks were

Table 5
Properties of the treated samples.

Mixture properties	$S_{44}A_4H_1$	$S_{54}A_{12}H_3$	$S_{64}A_{20}H_5$
Initial moisture content of untreated clay (%)	39	39	39
ACBFS (%)	4	12	20
IHL (%)	1	3	5
ACBFS-IHL to water ratio for producing the ACBFS-IHL slurry	1:1	1:1	1:1
Increase in mix moisture content due to adding slurry to paste clay (%)	5	15	25
Final moisture content of mixture before curing (%)	44	54	64

Fig. 3. Status of sample; (a) uncured sample in plexiglas mould, (b) samples being cured under a controlled curing pressure, (c) extruded sample after curing.

tested using the Brazilian tensile strength testing method.

4. Results and discussions

4.1. Initial unit weight and the equivalent depth of CSM panel

The initial saturated and dry unit weight of the samples ($\gamma_{s\text{-}int}$ and $\gamma_{d\text{-}int}$) were determined after filling the moulds with the mixtures and before curing. As shown in Table 6, adding the ACBFS-IHL slurry reduced both the initial saturated and dry unit weight of the mixtures. Previous research demonstrated that adding BFS powder to soil should increase the mixture's unit weight by filling the voids between soil particles (Akinmusuru, 1991; Wild et al., 1996; Rabbani et al., 2012). However, for the given additive contents in this research, the effect of lime and water has been the dominant factor in controlling the unit weight of the mixture. Therefore, despite the increase in ACBFS content, the total unit weight has decreased with increasing lime and water content.

The depth of CSM panels is usually between 2.5m to 21m depending on the project requirements (Fiorotto et al., 2006; Arnold et al., 2011). Knowing the saturated unit weight of the mixtures before curing as given in Table 6, the magnitude of the curing pressures in the oedometer cell is set in a way to represent the depth of the CSM panels with a depth varying from 6m to 24m (see Table 7).

4.2. Properties of the samples after curing

The samples were divided in two groups, one group extruded after 28 days and the other after 56 days of curing. To determine the unit weight of the cured samples (entire core), the samples were measured and weighted immediately after extruding. Moreover, a minimum of 25 g of each cured sample was cut for moisture content measurement by the use of a 110 ± 5 °C oven.

Fig. 4 presents the relationship between the applied curing pressure and the moisture content of the cured samples. As shown in this figure, after the curing process, the moisture content decreases due to an increase in the curing pressure. Although the pozzolanic reactions between the ACBFS and IHL influence the moisture content of the samples, the magnitude of curing pressure plays the main role in controlling the moisture content of the mixture during the curing process. The difference between the minimum and maximum moisture content for atmospheric pressure (zero curing pressure) is approximately 28%, while this difference decreases to 7% for 300–400kPa curing pressure. Also it can be seen that by increasing the curing pressure from 0 to 400kPa, the maximum drop in moisture content was 34.7% $\left(\frac{53.3-34.8}{53.3}\times 100\right)$ for the sample $S_{64}A_{20}H_5$ cured for 56 days, while the minimum drop was 19.1% $\left(\frac{41.8-33.8}{41.8}\times 100\right)$ for the sample $S_{44}A_4H_1$ cured for 28 days. In overall, it was observed that regardless of the amounts of ACBFS-IHL (from 5% to 25%) and the initial moisture content of the mixtures (from 44% to 64%) before curing, the final moisture content of the cured samples contain various percentage of additives were approximately 35% if the curing pressures are more than 300kPa (panels deeper than 18.1m).

Fig. 5 presents the effect of the curing pressure on the saturated unit weight of the cured samples. By comparing saturated unit weight of the mixture before curing (Table 6) with the saturated unit weight of the samples cured under atmospheric pressure, it can be seen that the curing action (curing time) have negligible effects on the saturated unit weight of samples under zero curing pressure. In other words, the chemical reactions between soil particles and additives in the absence of a curing pressure were not effective enough to change the soil matrix and increase the saturated unit weight of the samples. However, in the presence of a curing pressure, the saturated unit weight of samples increases considerably by increasing the curing pressure. Generally, while a disturbed

Table 6
Unit weight of the samples before curing.

Sample unit weight	Untreated clay	$S_{44}A_4H_1$	$S_{54}A_{12}H_3$	$S_{64}A_{20}H_5$
$\gamma_{s\text{-}int}$ (kN/m^3)	17.3	17.2	17.0	16.6
$\gamma_{d\text{-}int}$ (kN/m^3)	12.4	11.9	11.0	10.1

Table 7
Curing pressures and the equivalent depth of the CSM panel.

Pressures (kPa)	$S_{44}A_4H_1$	$S_{54}A_{12}H_3$	$S_{64}A_{20}H_5$	Average depth (m)
	Equivalent depth (m)			
0	0	0	0	0
100	5.8	5.9	6	5.9
200	11.6	11.8	12	11.8
300	17.4	17.6	18.1	17.7
400	23.3	23.5	24.1	23.6

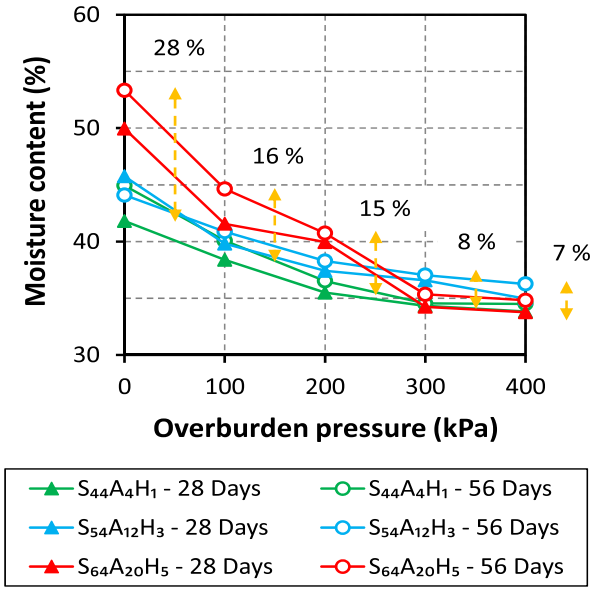

Fig. 4. Effect of curing pressures and curing time on the moisture content of cured samples.

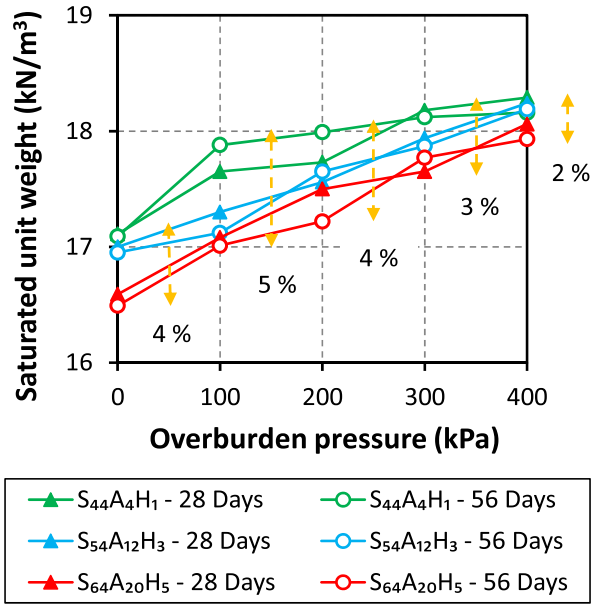

Fig. 5. Effect of curing pressures and curing time on the saturated unit weight of the cured samples.

clay sample is being consolidated, the primary consolidation happens relatively quickly during the first few hours of loading which has the major effect on controlling the size of voids between the clay particles as well as the unit weight. In contrast, the chemical reaction between the ACBFS and IHL is a prolonged process and usually requires several weeks to complete. It was also observed that by increasing the curing pressure from 0 to 400kPa, the maximum growth in saturated unit weight was 9% $\left(\frac{16.5-18}{16.5} \times 100\right)$ for the sample $S_{64}A_{20}H_5$ cured for 28 days, while the minimum growth was about 6.4% $\left(\frac{17-18.1}{17} \times 100\right)$ for the sample $S_{44}A_4H_1$ cured for 56 days.

Fig. 6 shows the effect of the curing pressure on the dry unit weight of the cured samples. Similar to the saturated unit weight, the dry unit weight of the cured samples is heavily controlled by the magnitude of the applied curing pressure. As illustrated in Fig. 6, all samples cured under 300kN and 400kN pressure showed almost the same dry unit weight with a maximum difference of 4% and 3% respectively. This is due to the fact that a considerable level of primary consolidation is achieved at such pressures which has resulted to denser soil matrix and higher dry unit weight regardless of the additive content and curing time. Therefore, in high curing pressure levels (i.e. more than 300kPa), the additives content (5% to 25%) and curing time (28–56 days) have marginal influence on changing the dry unit weight of the treated samples. As shown in Fig. 6, the maximum growth in dry unit weight due to increasing curing pressure from 0 to 400kPa was 24.2% $\left(\frac{10.7-13.3}{10.7} \times 100\right)$ for the sample $S_{64}A_{20}H_5$ cured for 56 days, while the minimum growth was 13.3% $\left(\frac{12-13.6}{12} \times 100\right)$ for the sample $S_{44}A_4H_1$ cured for 28 days.

According to the obtained results, it was found that the final saturated and dry unit weight of the cured samples consist of various percentage of additives were approximately 18.1 and 13.5 kN/m^3 respectively, if the curing pressures are more than 300kPa (panels deeper than 18.1m). Considering the relationship between the moisture content unit weight, usually the unit weight of a sample does not change if its moisture content reaches to a constant amount. Therefore, the obtained results in this section are consistent with the findings mentioned previously about the final moisture content of the cured samples.

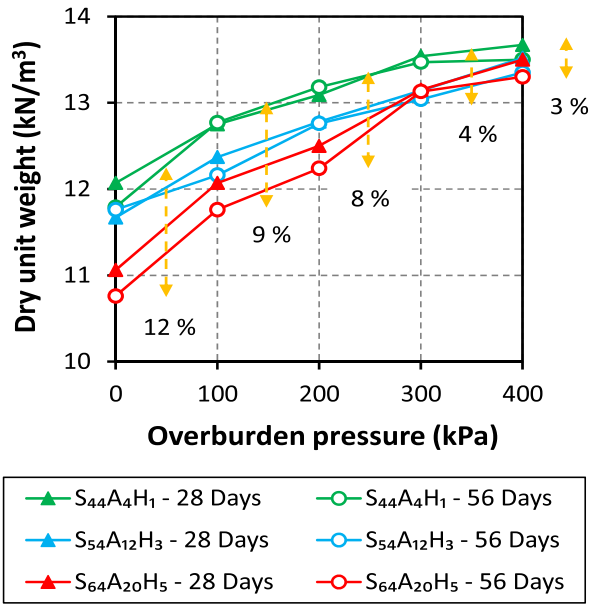

Fig. 6. Effect of curing pressure and curing time on the dry unit weight of cured samples.

4.3. Brazilian tensile strength test and results

4.3.1. Influence of the curing pressures and curing time on the tensile strength

The tensile strength of all the samples was measured by the Brazilian test method as shown in Fig. 7a. It should be mentioned that prepared Brazilian test disks from top, middle and bottom of the core had almost the same unit weight as the core (see section 4.2). Disks were gradually loaded by applying a controlled vertical displacement rate of 0.5 mm per minute until the tensile failure plane developed (see Fig. 8b). The maximum measured load was then translated into tensile strength using Eq. (1).

$$\sigma_t = 1.272\ P / \pi\ t\ D \quad (1)$$

where, σ_t is the material tensile strength (kPa), P is the maximum applied load (kN), t is the thickness of the sample (mm) and D is the diameter of the sample (mm).

A minimum of three samples for each additive level, curing time and curing pressure were tested, with the average magnitude of the tensile strength considered for comparison. Fig. 8 (a-d) shows the tensile strength results for the test conducted after 28 and 56 days of curing from various aspects of views. The effect of the treatment on the tensile

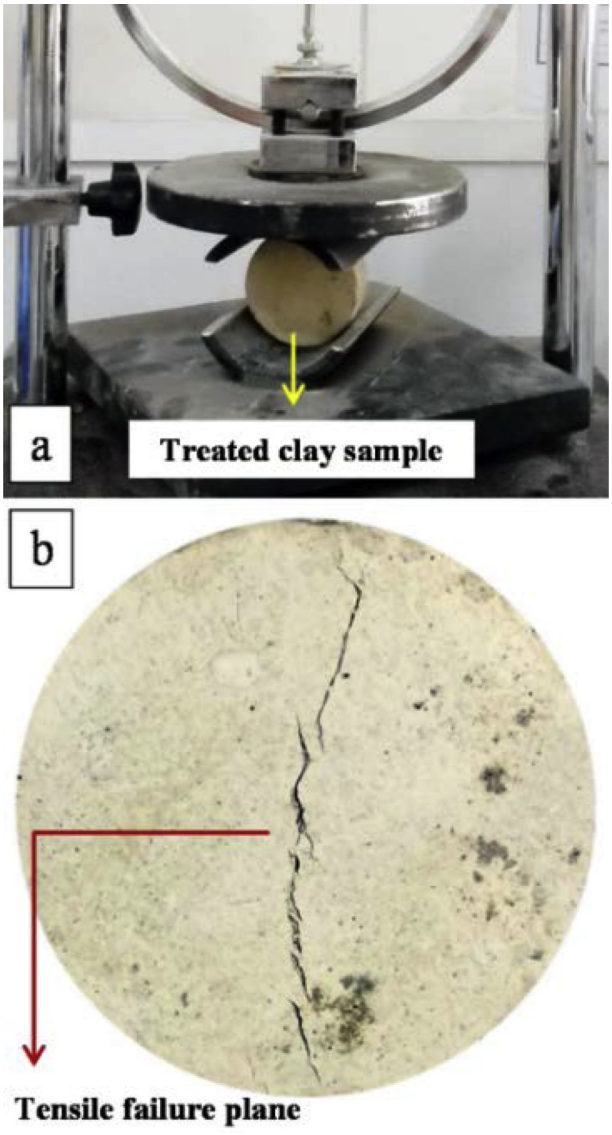

Fig. 7. Brazilian tensile strength test; (a) sample being tested (b) tension failure plane.

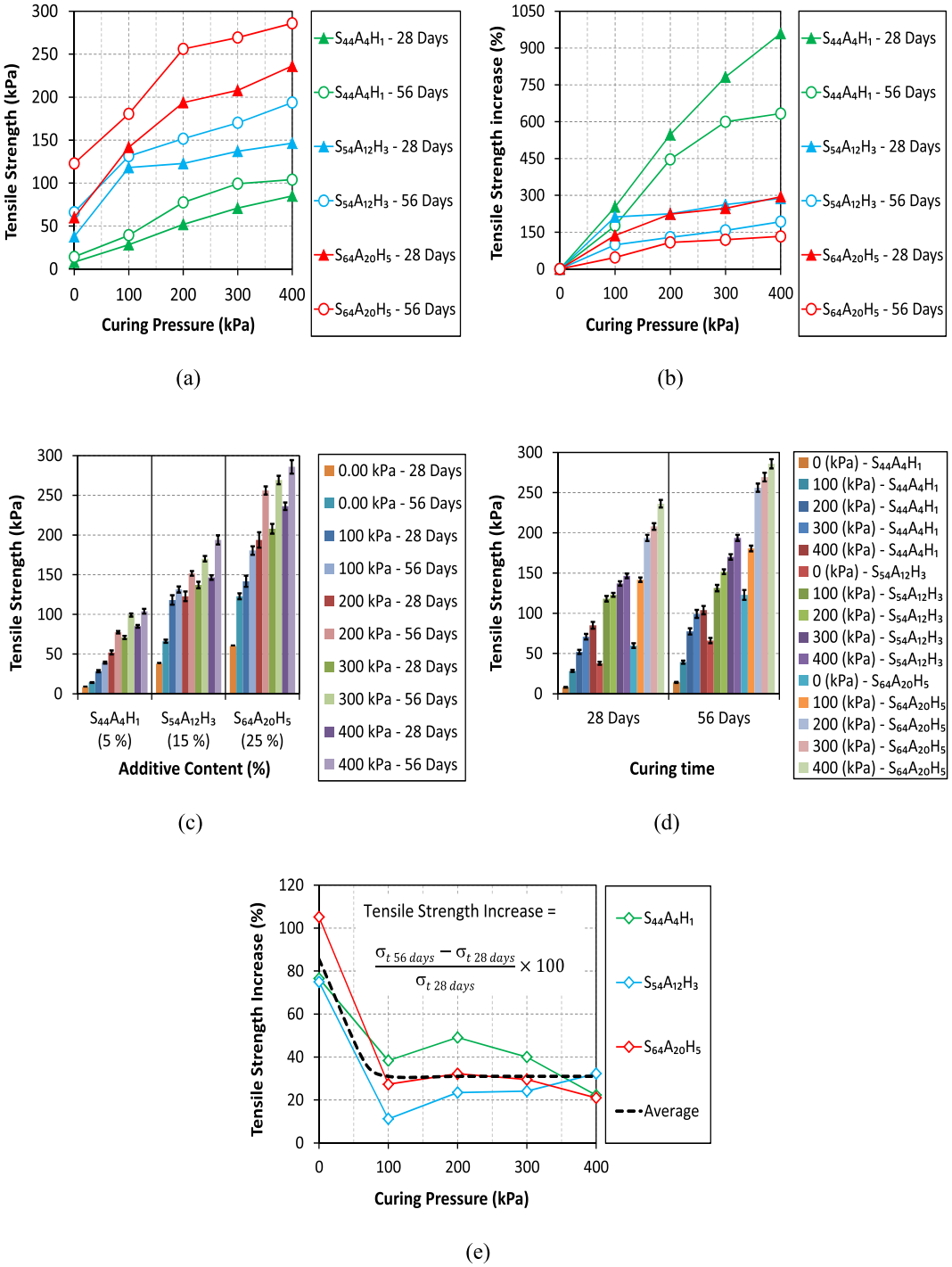

Fig. 8. Results of performed Brazilian tests; (a) the tensile strength of treated clay samples, (b) the growth rate of tensile strength by increasing the curing pressures, (c) the effect of additive content on the magnitude of the tensile strength, (d) the effect of curing time on the tensile strength of the treated clay, (e) the gain in the tensile strength when the curing time increases from 28 days to 56 days.

strength of the tested clay varies considerably. The minimum tensile strength after the treatment was about 8kPa for the $S_{44}A_4H_1$ samples cured for 28 days in the atmospheric pressure (zero curing pressure), while the maximum tensile strength was 286kPa for the $S_{64}A_{20}H_5$ samples cured for 56 days under 400kPa curing pressure.

Fig. 8a presents the effect of curing pressures on the tensile strength of the treated clay. As shown in this figure, by increasing the curing pressure the tensile strength of the samples increased considerably. It is obvious the greatest strength achieved at 400kPa curing pressures (23.6 m depth). Moreover, the strength-pressure diagrams illustrated sharp rise at the curing pressure between zero to 100kPa. However, by applying higher curing pressure (100–400kPa) trend decreased slightly.

Fig. 8b shows the growth rate of tensile strength by increasing the curing pressures in percentage terms, which actually indicates samples sensitivity to the applied curing pressures. This figure reports that the samples with different additive content (5%–25%) and curing time (28–56 days) show different sensitivities to curing pressures. The $S_{44}A_4H_1$ samples with the minimum amount of additives (5%) cured for 28 days showed the highest sensitivity with the 959% tensile strength growth if the curing pressure increases from 0kPa to 400kPa. In contrast,

the $S_{64}A_{20}H_5$ samples with maximum amount of additives (25%) cured for 56 days showed the least sensitivity to the applied curing pressure (0kPa–400kPa) with the 133% tensile strength growth. On average increasing curing pressures from zero to 400kpa increased the tensile strength of treated clay 417%.

Fig. 8c shows the effect of the additive content on the magnitude of tensile strength. Test results showed that the tensile strength of treated samples increases significantly with increasing ACBFS-IHL content. The $S_{64}A_{20}H_5$ sample consists of 25% additives and the $S_{44}A_4H_1$ samples with 5% additives showed the highest and lowest tensile strength respectively. On average, increasing additive content from 5% to 25% increased the tensile strength of treated clay 339%.

The effect of curing time on tensile strength is presented in Fig. 8d. It was observed that increasing the curing time from 28 to 56 days has led to increasing the tensile strength of treated clay. Fig. 8e indicates the gain in tensile strength (in percentage) when the curing time increases from 28 days to 56 days. Surprisingly, the samples cured at atmospheric pressure (zero curing pressure) are most sensitive to the curing time, as their tensile strength increases by 75%–105% (depending on the additive contents) when the curing time increases from 28 days to 56 days. However, the samples cured under pressure show similar sensitivity to the doubled up curing time. The change in the trend at the 100kPa curing pressure can be justified by taking the effect of voids into account. The existence of a positive curing pressure has decreased the voids between the clay particles and resulted in tensile strength gain to be less dependent on the curing time. With reasonable averaging, it is proposed that for all observed samples cured under an overburden pressure, the tensile strength increases by 30% when the curing time increases from 28 days to 56 days.

Considering the obtained results, three factors simultaneously contribute to an increase in the tensile strength of the tested clay. The first factor is the various curing pressures equivalent to different depths of the CSM panel, which causes consolidation and results in a denser geomaterial structure with fewer voids. The second factor is the chemical reactions due to mixing the clay with the slurries with different ACBFS-IHL contents. This usually includes pozzolanic reaction, flocculation, agglomeration, hydration and crystallisation of the treated clay, as a result of cation exchanges and the formation of new geomaterials with cementitious structures. The third factor is the curing time, which is literally the allocated time given for the chemical reactions as well as consolidation.

4.4. Microstructural analysis

To investigate the interaction of soft clay, ACBFS and IHL as well as their effect on tensile strength of treated clay from micro point of view, a set of microstructural tests were conducted. X-ray diffraction (XRD) patterns on the selected samples were determined from 5° and 90° (2θ), with a 0.02°/step using a Cu Kα radiation (Kα1 = 1.54059 Å; Kα2 = 154441 Å; Kα1/Kα2 = 0.497), at a scan rate of 3°/min operated at 45 kV and 40 mA "X'pert HighScore Plus" (PANalytical software) have been used for the identification of the present peaks. The untreated and treated clay with the highest and lowest tensile strengths were characterised by a field emission scanning electron microscope (FE-SEM) using a Zeiss Ultra Plus microscope. An accelerating voltage of 5 keV was used to investigate the structural and morphology of the selected samples. The samples were carbon coated with a 7–9 nm carbon layer.

Fig. 9 (a-c) shows the XRD patterns of (a), untreated clay, (b) treated clay with 4% ACBFS and 1% IHL (sample $S_{44}A_4H_1$) cured for 28 days at zero curing pressure and (c) the one contains 20% ACBFS and 5% IHL ($S_{64}A_{20}H_5$) cured for 56 days under 400kPa curing pressure (c). The graphs correspond to the treated samples with the highest and lowest tensile strength respectively. Quartz (SiO_2, JCPDS# 00-046-1045), calcite ($CaCO_3$, JCPDS# 00-005-0586), kaolinite ($Al_2Si_2O_5(OH)_4$, JCPDS# 00-29-1490), and muscovite (KAl1.91Fe0.09, JCPDS# 00-046-14099) were distinguished in all three samples, representing the nature of the clay. The XRD peaks in all three samples were related to quartz and kaolinite, respectively, which are the most abundant minerals of the untreated and treated samples, while the XRD planes were mostly related to muscovite and calcite representing lower amount of these minerals in the samples. It is obvious, no significant changes were detected in the XRD patterns of treated clay except a small peak of gismondine (possibly C–A–S–H) and calcium silicate hydrate (C–S–H) owing to the addition of a higher amount of ACBFS-IHL treated under 400kPa curing pressure. The C–A–S–H is identified at the peak of 32.6 A°, the formation of C–A–S–H in the system contains slag, lime and clay is common and mostly due to the presence of the slag particles. The presenting C–A–S–H is responsible for the strength development in a cementitious system and due to its strong chemical reaction. The improving effect of C–A–S–H on the strength of the treated clay with slag and lime has been reported by different researchers (Croft, 1967; James et al., 2008).

The SEM micrograph of untreated and treated clay is shown in Fig. 10 (a-f). SEM micrograph of the untreated clay (Figs. 10a and 10b) reveals a morphology showing a random array of sheet-like un-aggregated particles corresponding to the quartz, kaolinite and muscovite, the results are in agreement with the peaks that identified by XRD. The morphology of the treated clay with 4% ACBFS and 1% IHL (Figs. 10c and 10d) and the one contains 20% ACBFS and 5% IHL (Figs. 10e and 10f) show the formation of flocculated structure. The clusters interspersed by large openings are clearly visible in the treated sample with 4% ACBFS and 1% IHL as well as untreated clay. The treated clay also showed the platy nature, which was due to C-A-S-H as previously reported in the XRD

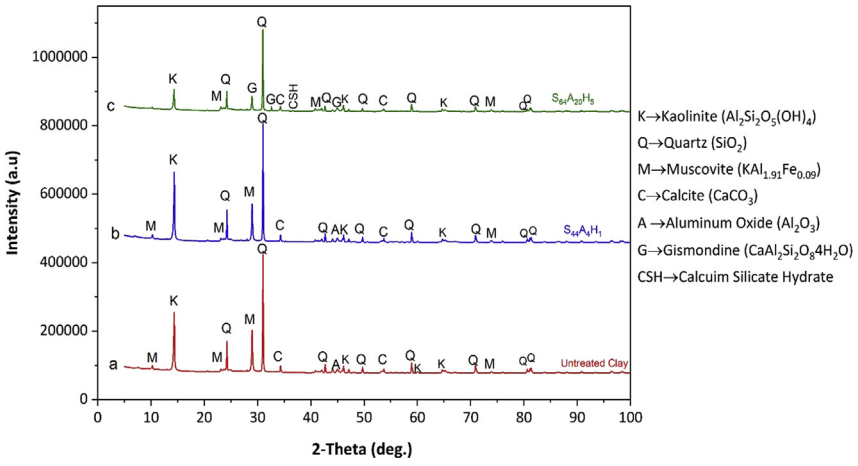

Fig. 9. X-ray diffraction patterns; (a) untreated clay, (b) treated clay with 4% ACBFS and 1% IHL cured for 28 days at zero curing pressure, (c) clay with 20% ACBFS and 5% IHL cured for 56 days at 400kPa curing pressure.

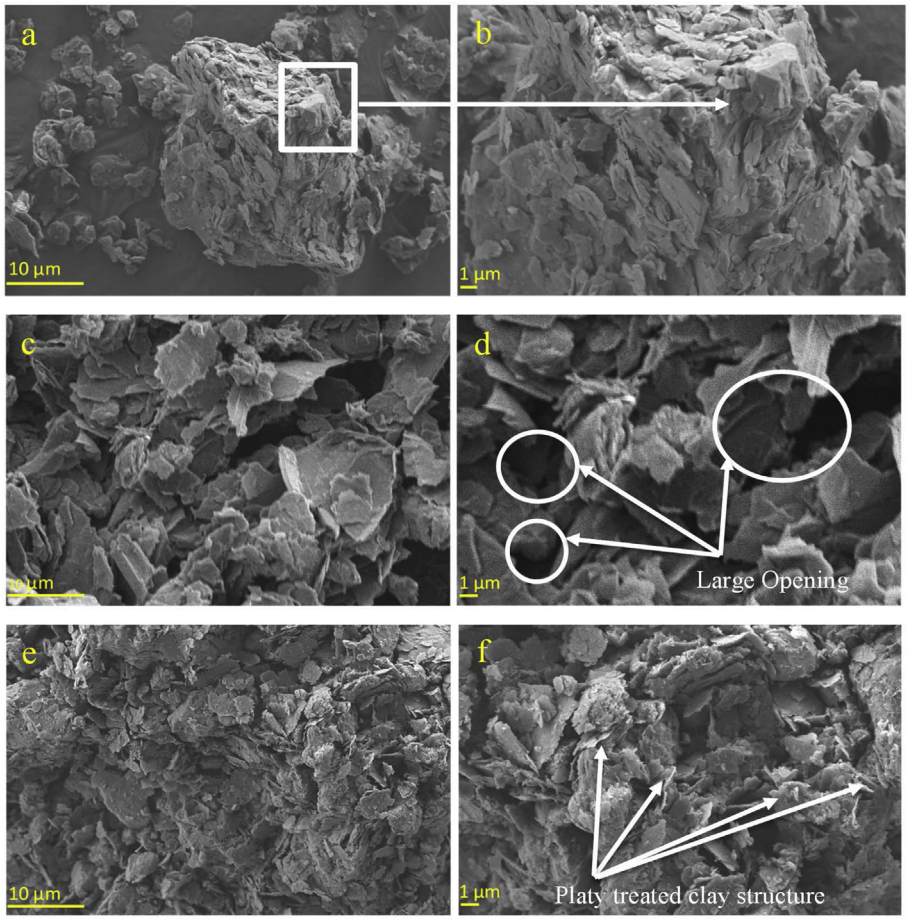

Fig. 10. SEM Micrographs of untreated and treated clay at different magnifications (×5k, right and ×10k, left) (a, b) untreated clay (c, d) treated clay with 4% ACBFS and 1% IHL cured for 28 days at zero curing pressure (e, f) treated clay with 20% ACBFS and 4% IHL cured for 56 days at 400kPa curing pressure.

analysis (James et al., 2008). The addition of ACBFS-IHL into the clay system has led to the formation of more flocculated structures and cementitious products and eventually the strength development as mentioned in section (4.3). Figs. 10e and 10f show the further progressing of the fluctuation process due to applying more pressure (400kPa) during 56 days of curing. Moreover, the effect of treatment is evident at higher pressures and ABCFS-IHL content by more compact structure due to the closing of macropores on their surface. Totally, treatment of clay with a higher amount of ABCFS-IHL has resulted in an increase in the tensile strength from about 8 to 286kPa after curing process which is due to the activity of the ACBFS with lime in enhancing pozzolanic reactions in the system (Falah et al., 2018; Rosone et al., 2018). The strength development can be described by the effect of ACBFS in hydration and pozzolanic reactions of the lime-treated clay up to 28-days curing periods. The crystalline cementitious products (such as C–A–S–H) formed via the pozzolanic reaction and diffusion of calcium ions (Ca^{2+}) in both lime and ACBFS particles. It should be noted that the effect of bridging or cementation in the pozzolanic reaction has a significant effect on the final strength. The XRD results also confirmed the formation of C–A–S–H in the sample contains higher amount of ACBFS. Moreover, the microstructure analysis of the final products showed a flocculated, dense and more crystalline structure with increasing in ACBFS content.

5. Conclusion

A laboratory-based attempt at evaluating the effect of CSM method, curing pressures (representing the mixing depth) and curing time on the tensile strength of a soft clay treated with ACBFS and IHL is reported in this study. Based on the finding obtained from different tests such as; consolidation test, Brazilian tensile test, XRD and SEM analysis the following conclusions were drawn from this investigation:

1. The moisture content of CSM panels decreases by 19.1–37% by increasing the curing pressures from zero to 400kPa (0m–23.6m mixing depth). However, the final moisture content of cured CSM panels with various percentages of additives was found to be almost 90% of the saturated moisture content of untreated clay under 300kPa curing pressure and more (panels deeper than 18.1m).
2. The saturated and dry unit weight of CSM panels increases by 6.4–9% and 13.3–24.2% respectivly, when the curing pressure increases from zero to 400kPa (0m–23.6m mixing depth). However, by applying 300kPa curing pressure and more (panels deeper than 18.1m), the final saturated and dry unit weight of CSM panels consist of various percentages of additives was found to be 105% and 109% of the saturated and dry unit weight of untreated clay respectively.
3. On average, by increasing the curing pressures (zero to 400kPa), the ACBFS-IHL content (5%–25%) and the curing time (28 days–56 days), the tensile strength of the CSM panels increases 417%, 339% and 30% respectively. However, simultaneous using of the CSM method and curing pressures along with ACBFS-IHL as a chemical stabiliser can increase the tensile strength of the CSM panels up to 35 times. In overall, the treated soil with 20% ACBFS and 5% IHL shows the highest tensile strength, depending on the curing pressures and curing time. Therefore, applying the mentioned proportion of additives is recommended for the construction of CSM panels. Moreover, as mentioned before, as the consequence of the materials self-weight the effect of treatment on the engineering properties and strength of the

treated soil varies at different depths. Such a variation should be taken into account at the design and construction stages.

4. By increasing the curing pressures from zero to 400kPa (0m–23.6m mixing depth), the growth of the tensile strength of the CSM panels with the minimum ACBFS-IHL content and curing time can be seven times more sensitive to the mixing depth than the CSM panels with the maximum ACBFS-IHL content and curing time (133%–959%). Moreover, significant changes on the physical properties of CSM panels including moisture content, saturated and dry unit weight occur at curing pressure less than 100kPa (0m–5.9m mixing depth).
5. The increase in the tensile strength of CSM panels from micro point of view is due to more compact structure of the CSM panels and closing of macropores on its surface as well as the pozzolanic reactions between the ACBFS and IHL that leads to formation of cementitious minerals such as C-A-S-H and C–S–H during curing time.

Declarations

Author contribution statement

Parham Rabbani: Performed the experiments; Analyzed and interpreted the data; Contributed reagents, materials, analysis tools or data; Wrote the paper.

Seyed Hamid Lajevardi & Ali Tolooiyan: Conceived and designed the experiments; Analyzed and interpreted the data; Contributed reagents, materials, analysis tools or data.

Younes Daghigh & Mahroo Falah: Analyzed and interpreted the data; Contributed reagents, materials, analysis tools or data.

Funding statement

This research did not receive any specific grant from funding agencies in the public, commercial, or not-for-profit sectors.

Competing interest statement

The authors declare no conflict of interest.

Additional information

No additional information is available for this paper.

Acknowledgements

The first author wishes to acknowledge the support provided by Keyhan-Khak Soil Mechanics and Concrete Co., Karaj, Iran, with the preparation of the equipment and help with laboratory testing for this research.

References

Abdel Rahman Ouf, M.E.S., 2001. Stabilisation of Clay Subgrade Soil Using Ground Granulated Ballast Furnace Slag. Doctor of Philosophy Thesis. University of Leeds, United Kingdom.

Addanki, V.G.K., Zdenek, E., Norbert, R.M., 1974. Behavior of compacted soil in tension. J. Geotech. Eng. Div. 100 (9), 1050–1061.

Akinmusuru, J.O., 1991. Potential beneficial uses of steel slag wastes for civil engineering purposes. Resour. Conserv. Recycl. 5 (1), 73–80.

Alrubaye, A.J., Hasan, M., Fattah, M.Y., 2017. Stabilization of soft kaolin clay with silica fume and lime. Int. J. Geotech. Eng. 11 (1), 90–96.

Arnold, M., Beckhaus, K., Wiedenmann, U., 2011. Cut-off wall construction using Cutter Soil Mixing: a case study. Geotechnik 34 (1), 11–21.

Arslan, H., Sture, S., Batiste, S., 2008. Experimental simulation of tensile behavior of lunar soil simulant JSC-1. Mater. Sci. Eng. A 478, 201–207.

ASTM D422 – 63, 2007. Standard Test Method for Particle-Size Analysis of Soils. D422 – 63. Reapproved 2007.

ASTM D698 – 12, 2012. Standard Test Methods for Laboratory Compaction Characteristics of Soil Using Standard Effort. D698 – 12.

ASTM D854 – 14, 2014. Standard Test Methods for Specific Gravity of Soil Solids by Water Pycnometer. D854 – 14.

ASTM D1633 - 00, 2007. Standard Test Methods for Compressive Strength of Molded Soil-Cement Cylinders, D1633-00.

ASTM D2166 - 16, 2016. Standard Test Method for Unconfined Compressive Strength of Cohesive Soil, D2166/D2166M – 16.

ASTM D2435/D2435M - 11, 2011. Standard Test Methods for One-Dimensional Consolidation Properties of Soils Using Incremental Loading. D2435/D2435M - 11.

ASTM D3967 – 16, 2016. Standard Test Method for Splitting Tensile Strength of Intact Rock Core Specimens. D3967 – 16.

ASTM D4318 – 10, 2010. Standard Test Methods for Liquid Limit, Plastic Limit, and Plasticity Index of Soils. D4318 – 10.

Axelsson, K., Johansson, S.E., Andersson, R., 2002. Stabilisation of Organic Soils by Cement and Pozzolanic Reactions" Report 3, Feasibility Study (Pp. P 54): Swedish Deep Stabilisation Research Centre, C/o Swedish Geotechnical Institute.

Bauer Maschinen GmbH, 2016. Process Description Manual; Cutter Soil Mixing Process and Equipment" 905.656.2 (905.656.2 ed.). BAUER Foundation Corp, Germany.

Bell, F.G., Culshaw, M.G., 2001. Problems soils: a review from a British perspective. In: Paper Presented at the Problematic Soils Symposium, Nottingham, UK.

Bellato, D., Simonini, P., Marzano, I.P., Leder, E., Grisolia, M., Vohs, T., Gerressen, F.W., 2012. Mechanical and physical properties of a CSM cut-off/retaining wall. In: Paper Presented at the ICGI 2012 - International Conference on Ground Improvement and Ground Control. Wollongong, Australia.

Bhuyan, S., Singh, S.P., 2010. Stabilisation of Balast Furnace Slag and Fly Ash Using Lime and Rbi Grade 81". (Bachelor's Degree). National Institute of Technology, Rourkela, India.

Bruce, D.A., 2009. Seepage cut-offs for levees and dams: the technology review. In: Paper Presented at the Dam Safety Annual Conference Hollywood, Florida, USA.

Bruce, M.E.C., Berg, R.R., Collin, J.G., Filz, G.M., Terashi, M., Yang, D.S., 2013. Federal Highway Administration Design Manual: Deep Mixing for Embankment and Foundation Support" (U. S. D. O. Transportation, Trans.) FHWA-HRT-13-046 (FHWA-HRT-13-046 ed., Pp. 244). U.S Department of Transportation, Federal Highway Administration Design Manual, USA.

Brunner, W., Fiorotto, R., Stötzer, E., Schöpf, M., 2006. The innovative CSM-cutter soil mixing for constructing retaining and cut-off walls. In: Paper Presented at the Geotechnical Engineering in the Information Technology Age: Proceedings of GeoCongress 2006, Atlanta, Georgia, United States.

Budhu, M., 2008. Soil Mechanics and Foundations(with CD). Wiley India Pvt. Limited, New York, United States.

Chai, J., Carter, J.P., 2011. Deformation Analysis in Soft Ground Improvement. Springer.

Chen, J., Anandarajah, A., Inyang, H., 2000. Pore fluid properties and compressibility of kaolinite. J. Geotech. Geoenviron. Eng. 126 (9), 798–807.

Croft, J.B., 1967. The influence of soil mineralogical composition on cement stabilization. Geotechnique 17, 119–135.

Denies, N., Huybrechts, N., De Cock, F., Lameire, B., Maertens, J., bvba, J.M., . . . Leuven, K., 2012. Soil mix walls as retaining structures – Belgian practice. In: Paper Presented at the ISSMGE - TC 211 International Symposium on Ground Improvement, Brussels, Belgium.

Falah, M., RanjbarPouya, K., Tolooiyan, A., Mackenzie, K., 2018. Structural behaviour of an Australian silty clay (coode island silt) stabilised by treatment with slag lime. Appl. Clay Sci. 157 (1).

Fang, H.Y., 1997. Introduction to Environmental Geotechnology. CRC Press, USA.

FHWA-RD-97-148, 2016. User Guidelines for Waste and Byproduct Materials in Pavement Construction" (U. S. D. O. Transportation, Trans.) FHWA-RD-97-148. Federal Highway Administration, U.S Department of Transportation, USA.

Fiorotto, R., Schöpf, M., Stötzer, E., 2005. Cutter soil mixing (CSM) - an innovation in soil mixing for creating cut-off and retaining walls. In: Paper Presented at the Proceedings of the 16th International Conference on Soil Mechanics and Geotechnical Engineering, Osaka-Japan.

Fiorotto, R., Schöpf, M., Stötzer, E., 2006. Cutter Soil Mixing (C.S.M.) an innovation in soil mixing for creating cut-off and retaining walls. In: Proceedings of the 16th International Conference on Soil Mechanics and Geotechnical Engineering, pp. 1185–1188.

Gerressen, F., Vohs, T., 2012. CSM-cutter soil mixing—worldwide experiences of a young soil mixing method. In: Paper Presented at the Grouting and Deep Mixing 2012, Proceedings of the 4th International Conference on Grouting and Deep Mixing, New Orleans, Louisiana, United States.

Güllü, H., Canakci, H., Al Zangana, I.F., 2017. Use of cement based grout with glass powder for deep mixing. Constr. Build. Mater. 137, 12–20.

Higgins, D.D., 2005. Soil Stabilisation with Ground Granulated Blast Furnace Slag" (Pp. P 15): UK Cementitious Slag Makers Association (CSMA).

Higgins, D.D., Kinuthia, J.M., Wild, S., 1998. Soil stabilisation using lime-activated GGBS. In: Paper Presented at the Proceedings of the 6 Th ACI/CANMET International Conference on Fly Ash, Silica Fume, Slag and Natural Pozzolans in Concrete, Bangkok, Thailand.

Hudson, W.R., Kennedy, T.W., 1968. An Indirect Tensile Test for Stabilized Materials" Evaluation of Tensile Properties of Subbases for Use in New Rigid Pavement Design-No. 98-1. The Texas Highway Department, The University of Texas at Austin.

Huertas, F.J., Fiore, S., Huertas, F., Linares, J., 1999. Experimental study of the hydrothermal formation of kaolinite. Chem. Geol. 156, 171–190.

James, R., Kamruzzaman, A.H.M., Haque, A., Wilkinson, A., 2008. Behaviour of lime–slag-treated clay. In: Proceedings of the Institution of Civil Engineers - Ground Improvement, 161, pp. 207–216.

Jamsawang, P., Boathong, P., Mairaing, W., Jongpradist, P., 2016a. Undrained creep failure of a drainage canal slope stabilized with deep cement mixing columns. Landslides 13 (5), 939–955.

Jamsawang, P., Voottipruex, P., Boathong, P., Mairaing, W., Horpibulsuk, S., 2015. Three-dimensional numerical investigation on lateral movement and factor of safety of slopes stabilized with deep cement mixing column rows. Eng. Geol. 188, 159–167.
Jamsawang, P., Yoobanpota, N., Thanasisathita, N., Voottipruex, P., Jongpradist, P., 2016b. Three-dimensional numerical analysis of a DCM column-supported highway embankment. Comput. Geotech. 72, 42–56.
Jamsawanga, P., Nuansrithongb, N., Voottipruexc, P., Songpiriyakijd, S., Jongpradiste, P., 2017. Laboratory investigations on the swelling behavior of composite expansive clays stabilized with shallow and deep clay-cement mixing methods. Appl. Clay Sci. 148, 83–94.
Kabasy, M.A.E.M., 2013. Improvement of swelling clay properties using hay fibers. In: Paper Presented at the Construction and Building Materials.
Kamon, M., Bergado, D.T., 1991. Ground improvement techniques. In: Paper Presented at the Proceedings of the 9th Asian Regional Conference on Soil Mechanics and Foundation Engineering, Bangkok, Thailand.
Kempfert, H.G., Gebreselassie, B., 2006. Excavations and Foundations in Soft Soils. Springer, Berlin, Heidelberg, 591 p.
Keramatikerman, M., Chegenizadeh, A., Nikraz, H., 2016. Effect of GGBFS and lime binders on the engineering properties of clay. Appl. Clay Sci. 132–133, 722–730.
Kim, T.H., Kim, T.H., Kang, G.C., Ge, L., 2012. Factors influencing crack-induced tensile strength of compacted soil. Journal of Materials in Civil Eengineering 24 (3), 315–320.
Kitazume, M., Maruyama, K., 2007. Internal stability of group column type deep mixing improved ground under embarkment loading. Soils Found. 47 (3), 437–455.
Kitazume, M., Terashi, M., 2017. The Deep Mixing Method. CRC press, 410 p.
Li, J., Tang, C., Wang, D., Pei, X., Shi, B., 2014. Effect of discrete fibre reinforcement on soil tensile strength. In: Paper Presented at the Journal of Rock Mechanics and Geotechnical Engineering.
Manso, J.M., Ortega-López, V., Polanco, J.A., Setién, J., 2013. The use of ladle furnace slag in soil stabilization. In: Paper Presented at the Construction and Building Materials.
Mohamedzein, Y.E.A., AL-Aghbari, M.Y., Taha, R.A., 2006. Stabilisation of desert sands using municipal solid waste incinerator ash. Geotech. Geol. Eng. 24 (6), 1767–1780.
Moore, D.M., Reynolds, R.C., 1998. X-ray diffraction and identification and analysis of clay minerals. Geol. Mag. 135, 819–842.
Nazari, A., Riahi, S., 2011. The role of SiO2 nanoparticles and ground granulated blast furnace slag admixtures on physical, thermal and mechanical properties of self compacting concrete. Mater. Sci. Eng. A 528, 2149–2157.
Nelson, J.D., Miller, D.J., 1992. Expansive Soils, Problems and Practice in Foundation and Pavement Engineering. Wiley, New York.
Nguyen, B., Takeyama, T., Kitazume, M., 2016. Internal failure of deep mixing columns reinforced by a shallow stabilized soil beneath an embankment. In: Paper Presented at the Int. J. Of Geosynth. and Ground Eng.
Nicholson, P.J., Mitchell, J.K.H., Bahner, E.W., Moriwaki, Y., 1998. Design of a Soil Mixed Composite Gravity Wall" (Pp. P 15). American Society of Civil Engineers, Rutgers, New Jersey. United States. Presented at.
Obuzor, G.N., Kinuthia, J.M., Robinson, R.B., 2012. Soil stabilisation with lime-activated-GGBS—a mitigation to flooding effects on road structural layers/embankments constructed on floodplains. Eng. Geol. 151, 112–119.
Oliveira, P.J.V., Pinheiro, J.L.P., Correia, A.A.S., 2011. Numerical analysis of an embankment built on soft soil reinforced with deep mixing columns: parametric study. Comput. Geotech. 38, 566–576.
Rabbani, P., Daghigh, Y., Atrechian, M.R., Karimi, M., Tolooiyan, A., 2012. The potential of lime and Grand granulated blast furnace slag (GGBFS) mixture for stabilisation of desert silty sands. J. Civ. Eng. Res. 2 (6), 108–119.
Rahmat, M.N., Ismail, N., Kinuthia, J.M., 2016. Strength and environmental evaluation of stabilised clay-PFA eco-friendly bricks. Constr. Build. Mater. 125, 964–973.
Regourd, M., 1980. Structure and behavior of slag portland cement hydrates. In: Paper Presented at the Proceedings of the 7th International Congress on the Chemistry of Cement, Paris, France.
Rosone, M., Celauro, C., Ferrari, A., 2018. Microstructure and shear strength evolution of a lime-treated clay for use in road construction. In: International Journal of Pavement Engineering.
Rutherford, C., Biscontin, G., Briaud, J.L., 2005. "Design Manual for Excavation Support Using Deep Mixing Technology" (Pp. 211). Texas A&M University.
Saji, S., Numakarni, K., 1996. Reinforcement effect of composite earth retaining wall system on releasing strut. In: Paper Presented at the Geotechnical Aspects of Underground Construction in Soft Ground. Balkema, Rotterdam.
Sargent, P., Hughes, P.N., Rouainia, M., White, M.L., 2013. The use of alkali activated waste binders in enhancing the mechanical properties and durability of soft alluvial. Eng. Geol. 15 (1), 96–108.
Sargent, P., Hughesb, P.N., Rouainiac, M., 2016. A new low carbon cementitious binder for stabilising weak ground conditions through deep soil mixing. Soils Found. 56 (6), 1021–1134.
Shao, Y., Macari, E.J., Cai, W., 2005. Compound deep soil mixing columns for retaining structures in excavations. J. Geotech. Geoenviron. Eng. 131 (11), 1370–1377.
Shen, S.L., Han, J., Du, Y.J., 2008. Deep mixing induced property changes in surrounding sensitive marine clays. J. Geotech. Geoenviron. Eng. 134 (6), 845–854.
Shindea, S.B., Kalaa, V.U., Kadalia, S., Tirumkudulub, M.S., Singha, D.N., 2012. A novel methodology for measuring the tensile strength of expansive clays. Geomech. Geoeng. Int. J. 7 (1), 15–25.
Smolczyk, H.G., 1980. Slag structure and identification of slag. In: Paper Presented at the Proceedings of the 7th International Congress on the Chemistry of Cement, Paris, France.
Thompson, M.R., 1965. The Split-Tensile Strength of Lime-Stabilized Soils" Lime Stabilization (Vol. Highway Research Record No. 92, Pp. Pp 69-79): Highway Research Board.
Tolooiyan, A., Gavin, K., 2011. Modelling the cone penetration test in sand using cavity expansion and arbitrary Lagrangian eulerian finite element methods. Comput. Geotech. 38, 482–490.
Tolooiyan, A., Mackay, R., Xue, J., 2014. Measurement of the tensile strength of organic soft rock. Geotech. Test J. 37 (6), 991–1001.
Wagner, J.F., 2013. In: Bergaya, F., Lagaly, G. (Eds.), Developments in Clay Science, Chapter 9 - Mechanical Properties of Clays and Clay Minerals. Elsevier, pp. 347–381.
Wild, S., Kinuthia, J.M., Robinson, R.B., Humphreys, I., 1996. Effects of ground granulated blast furnace slag (GGBS) on the strength and swelling properties of lime - stabilised kaolinite in the presence of sulphates. Clay Miner. J. Fine Part. Sci. 31 (3), 423–433.
Wild, S., Tasong, W.A., 1999. Influence of ground granulated blast furnace slag on the sulphate resistance of lime-stabilised kaolinite. Mag. Concr. Res. 51 (4), 247–254.
Wonglert, A., Jongpradist, P., 2015. Impact of reinforced core on performance and failure behavior of stiffened deep cement mixing piles. Comput. Geotech. 69, 93–104.
Xiaolin, Y., Jiaa, B., 2012. Analysis of excavating foundation pit to nearby bridge foundation. Procedia Earth Planet. Sci. 5, 102–106.
Yi, Y., Gu, L., Liu, S., 2015. Microstructural and mechanical properties of marine soft clay stabilized by lime-activated ground granulated blastfurnace slag. Appl. Clay Sci. 103, 71–76.
Zegeye, A., Yahaya, S., Fialips, C.I., White, M.L., Gray, N.D., Manning, D.A.C., 2013. Refinement of industrial kaolin by microbial removal of iron-bearing impurities. Appl. Clay Sci. 86, 47–53.